Carbon−Nitrogen Place Exchange on NO Exposed β-Mo_2C

Mohamed Siaj,[†] Carl Maltais,[†] El Mamoune Zahidi,[†] Hicham Oudghiri-Hassani,[†] Jiqing Wang,[†] Federico Rosei,[‡] and Peter H. McBreen*,[†]

Département de chimie, Université Laval, Québec (Qc), Canada G1K 7P4, and INRS-EMT, 1650 Boul. Lionel Boulet, Varennes (Qc), Canada J3X 1S2

Received: April 6, 2005; In Final Form: June 13, 2005

Atomic nitrogen and oxygen were deposited on β-Mo_2C through dissociative adsorption of NO. Reflectance absorbance infrared spectroscopy (RAIRS), thermal desorption, and synchrotron X-ray photoelectron spectroscopy (XPS) measurements were used to investigate the interplay between atomic nitrogen, carbon, and oxygen in the 400−1250 K region. The combination of the high resolution and high surface sensitivity offered by the synchrotron XPS technique was used to show that atomic nitrogen displaces interstitial carbon onto the carbide surface. Thermal desorption measurements show that the burnoff of the displaced carbon occurs at approximately 890 K. The incorporation of nitrogen into interstitial sites inhibits oxygen dissolution into the bulk. RAIRS spectroscopy was used to identify surface oxo, terminal oxygen, species formed from O_2 and NO on β-Mo_2C.

Introduction

Experimental[1−12] investigations of the surface properties and reactivity of group 6 carbides have been carried out extensively. The chemisorption properties, catalytic activity, and selectivity of these compound materials depend sensitively on the surface atomic composition. For pure carbides, the chemisorption properties depend critically on how the carbon is distributed in the surface region. For example, molybdenum carbide model catalysts can be rendered as reactive as Pt or Ru by heating to 1200 K to drive excess carbon into the subsurface.[11] The carbon-to-metal ratio at the surface of carbides, and the nature of the surface carbon, depends on the method of synthesis[13−17] and on the depletion or accumulation of carbon due to interaction with gas-phase molecules. Changes in the carbon-to-metal ratio can occur spontaneously under reaction conditions as in the induction period for methane aromatization on Mo/ZSM-5 catalysts.[18,19] The formation of interstitial molybdenum carbide leads to charge transfer to carbon, the expansion of the molybdenum lattice, and metal−carbon covalent bonding.[20] Excess carbon on the surface is expected to lead to site blocking. Liu and Rodriguez have presented calculations showing that the reactivity of metal carbide systems can vary as a complex function of the metal-to-carbon ratio.[20]

In this study, we use nitric oxide (NO) as a probe molecule to dose the carbide surface with atomic nitrogen and oxygen. By using the high surface sensitivity and high resolution possible with synchrotron X-ray photoelectron spectroscopy (XPS), we are able to follow the complex set of atomic displacements which occur as N and O are added to the surface and subsequently removed in desorption steps. It is well-known that adding oxygen to carbide surfaces can cause marked changes in their chemical reactivity. For example, modification of molybdenum carbide catalysts with surface oxygen induces changes in selectivity from hydrogenolysis toward isomerization.[21,22] Treatment with oxygen at elevated temperatures can lead to the removal of interstitial carbon. Carbon removal is observed even at low temperatures during the interaction of O_2 or H_2O with titanium carbide.[23−25] A number of studies have reported on the adsorption of NO on molybdenum and tungsten carbides.[26−28] Zhang et al. have studied the interaction of NO with a carbide W(111) surface and with a layer of Mo/C on W(111).[29,30] They found that the interaction of NO with both surfaces leads to removal of carbon in a high-temperature CO desorption peak. In a previous study, we reported preliminary XPS and thermal desorption data consistent with the cooperative replacement of carbide carbon with nitrogen in the NO dissociation/N_2 and CO desorption cycle on β-Mo_2C.[27]

Experiment

Vibrational spectroscopy and thermal desorption experiments were performed in an ultrahigh-vacuum system equipped for reflectance absorbance infrared spectroscopy (RAIRS), temperature-programmed desorption (TPD), and conventional XPS measurements. The base pressure of the chamber was 4×10^{-11} Torr. The interstitial carbide was prepared by Oyama and Ramanathan by carburizing pure molybdenum foil in a flowing 20% CH_4/H_2 mixture using the temperature ramp method. X-ray diffraction (XRD) analysis showed the sample to be pure bulk β-Mo_2C.[31] The clean sample displayed an XPS determined Mo/C atomic ratio of 2:1. A tantalum foil support was used to mount the polycrystalline β-Mo_2C sample, by curving its extremities around the carbide. The Ta foil was, in turn, spot-welded to two tantalum wires that spanned two electrical feedthroughs mounted on a reservoir for liquid N_2. In this arrangement, the sample could be cooled to ~100 K by thermal contact with the liquid nitrogen reservoir and heated to 1450 K by resistive heating. The temperature was measured using a chromel−alumel thermocouple that was spot-welded to the tantalum support. The high temperature readings were verified using an optical pyrometer. The β-Mo_2C sample was cleaned by repeated cycles of Ar^+ sputtering at 500 K to remove sulfur.

* Corresponding author.
[†] Université Laval.
[‡] INRS-EMT.

10.1021/jp051776v CCC: $30.25
Published on Web 07/22/2005

Residual surface oxygen was minimized by exposing the sample to ethene or propene at 500−600 K and heating to 1400 K.

High-resolution, surface-sensitive XPS measurements were performed using the SuperESCA beamline at ELETTRA, the third generation synchrotron radiation source in Trieste.[32] Photoelectrons were collected at 70° with respect to the surface normal. To further ensure high surface sensitivity, we used the following photon energies: 400 eV, C(1s) and Mo(3d); 650 eV, O(1s); 500 eV, N(1s). The same sample preparation procedures were used for the RAIRS, TPD, and synchrotron studies. The lowest sample temperature was 86 K.

Results and Discussion

Atomic nitrogen and oxygen were dosed onto the β-Mo_2C surface through NO dissociation. The dissociation process, which occurs in the 86−400 K temperature range, was monitored by high-resolution N(1s) and O(1s) measurements (Figures 1 and 2). The N(1s) peaks at 400.2 and 397.3 eV can be readily assigned to chemisorbed NO[30,33,34] and atomic nitrogen,[30,33,35] respectively, indicating that some decomposition occurs even at 86 K. Heating the sample to 400 K causes the disappearance of the peak at 400.2 eV. This is consistent with RAIRS data showing the complete dissociation of a chemisorbed layer of NO on β-Mo_2C by ∼400 K.[26] This paper focuses on the fate of the resultant atomic O and N species, and their interplay with surface carbon, over the 400−1250 K temperature range. We will first discuss the O(1s) data. Two peaks located at 530.2 and 531.5 eV are observed over the high-temperature region. RAIRS data (Figures 3 and 4) will be used as an aid in interpreting the O(1s) spectra.

The RAIRS data in Figures 3 and 4 show that one of the O(1s) peaks may be attributed to surface oxo, Mo═O. In particular, Figure 3 shows a comparison of RAIRS spectra for dissociated O_2 (left panel) and ^{15}NO (right panel). Dissociative adsorption of O_2 gives rise to a band at 941 cm^{-1}, with a shoulder toward higher frequencies, whereas the spectrum arising from NO dissociation displays a band at 989 cm^{-1} and a shoulder at 942 cm^{-1}. Since identical spectra (Figure 4) are obtained using ^{15}NO and ^{14}NO, the observed signal cannot be attributed to a molybdenum−nitrogen vibrational mode. In contrast, the band at 990 cm^{-1} may be readily attributed to Mo═O by reference to several reports in the literature.[36−43] On-top oxygen (oxo) on molybdenum surfaces is usually characterized by a stretching frequency in the 960−1020 cm^{-1} range. Although the feature at 941 cm^{-1} is at an atypically low frequency for a surface oxo species, it is very close to values observed for single Mo atom oxo, $[Mo^{V}OS_4]^{-1}$, complexes.[44]

The high-resolution O(1s) spectra (Figure 2) display a dominant peak at 530.2 eV and a smaller contribution at 531.5 eV over the 400−1110 K range. Edamoto et al. reported O(1s) data for O_2 dissociation on α-Mo_2C(0001) at 300 K.[45] Their spectra display a principal peak at 530.1 eV and a shoulder at higher binding energy in the 531.5−532.0 eV region. Diener et al. reported that oxygen on Mo(110) is characterized by a peak at 530.9 eV and a satellite at 532.5 eV.[43] The low-binding-energy peak in each case may be readily attributed to high-coordination atomic oxygen. The high-binding-energy peak in Figure 2 is assigned to surface oxo on the basis of the RAIRS data. This conclusion may be compared to literature data for oxygen on VC(100).[23] The latter system shows an intense high-resolution electron energy loss spectroscopy (HREELS) loss due to surface oxo and an O(1s) binding energy of 530.0 eV with a tail toward higher binding energy. Examples of the coexistence of high-coordination and oxo species on molybdenum were

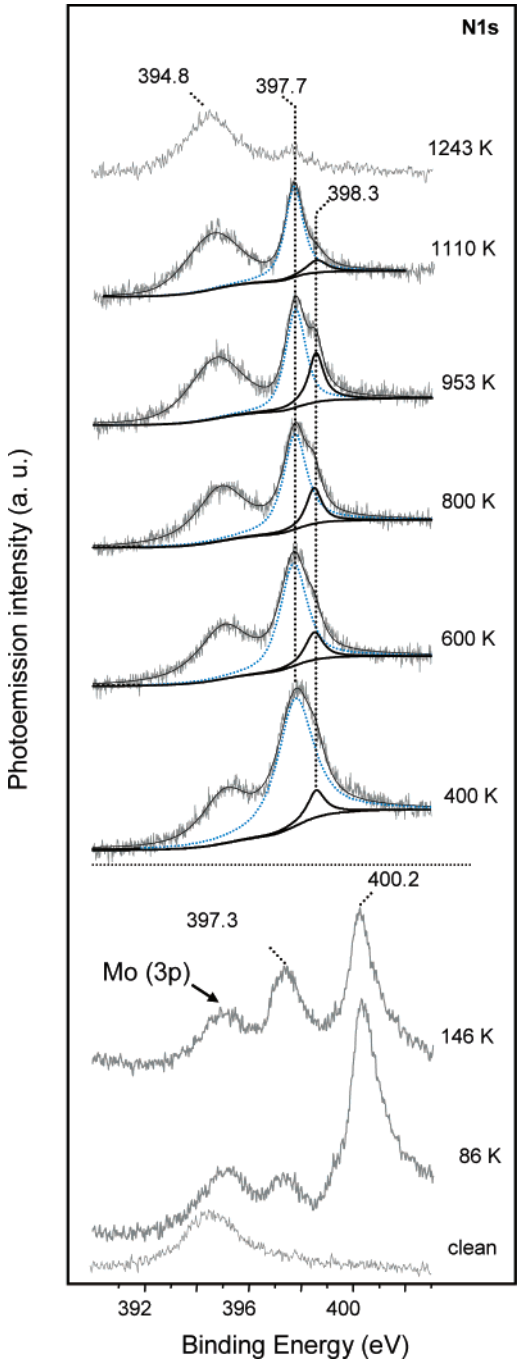

Figure 1. High-resolution N(1s) spectra for NO on β-Mo_2C. The sample was exposed to 5 L of NO at 86 K and then progressively annealed to the indicated temperatures. All spectra were recorded at the indicated temperatures.

reported by Friend et al.[42] They observed the facile exchange between on-top and high-coordination oxygen on Mo(110) even at 100 K and estimated a diffusion barrier height of 0.26 eV for the on-top to high-coordination site conversion. In a separate study, they observed that ^{16}O from nitromethane dissociation displaces ^{18}O from high-coordination into on-top sites in the 500−800 K range. Similarly, they observed that NO adsorption removes the oxo signal (1016 cm^{-1}) arising from step-edge sites, and subsequent NO desorption at 760 K leads to the reappearance of the oxo state.[46] Additional studies in our group show that the vibrational band of surface oxo prepared by O_2 dissociation on β-Mo_2C is still present after annealing to 1000 K. This is consistent with the data in Figure 2 showing the presence of the O(1s) peak at 531.5 eV at 1000 K. The latter

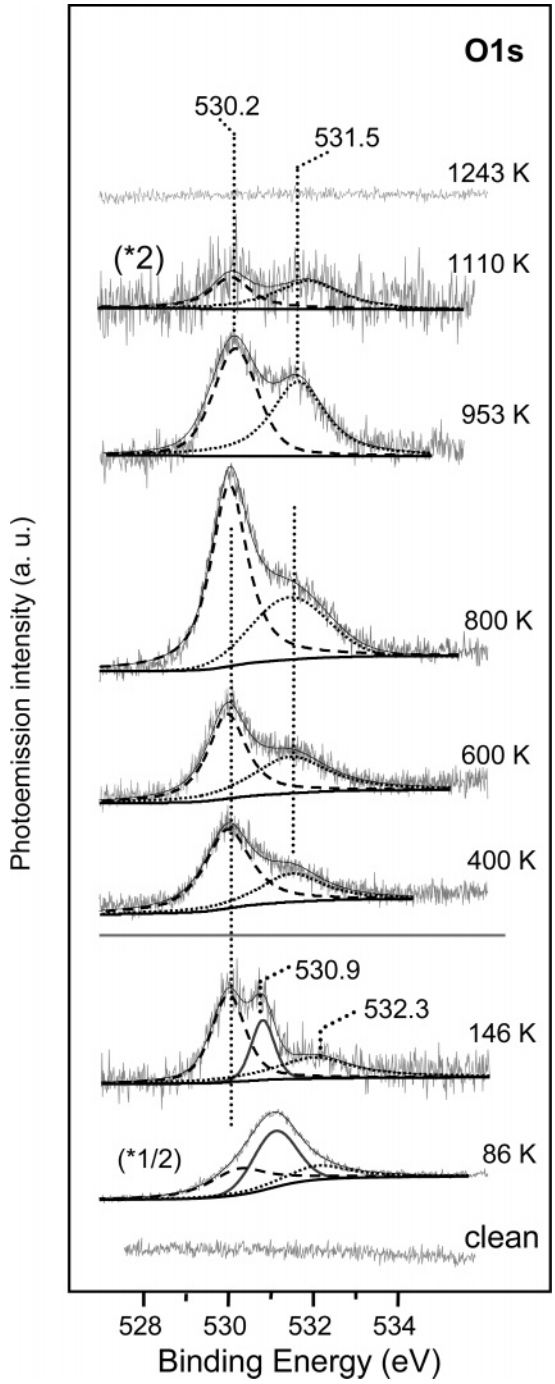

Figure 2. High-resolution O(1s) spectra for NO on β-Mo_2C. The sample was exposed to 5 L of NO at 86 K and then progressively annealed to the indicated temperatures. All spectra were recorded at the indicated temperatures.

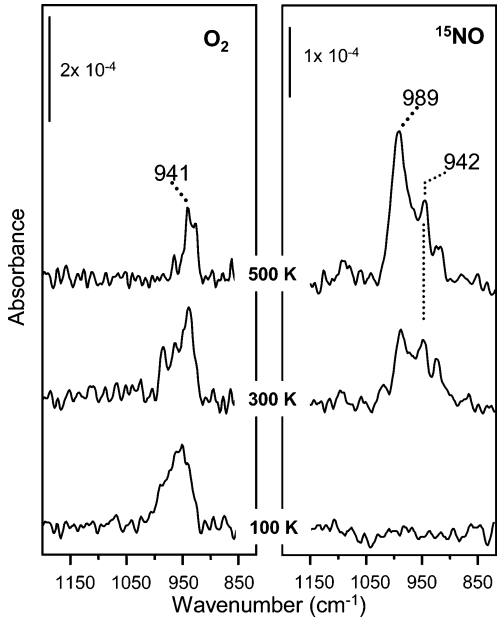

Figure 3. RAIRS spectra for (left panel) 0.5 L of O_2 and (right panel) 5 L of ^{15}NO on β-Mo_2C. All gas exposures and RAIRS measurements were carried out at 105 K.

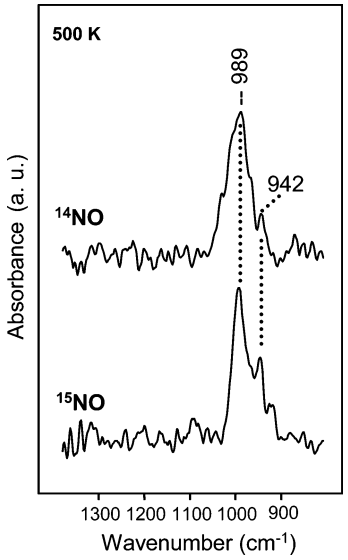

Figure 4. RAIRS spectra for ^{15}NO and ^{14}NO dissociation on β-Mo_2C. Exposures to 5 L were carried out at 105 K, and the spectra were recorded at 105 K following an anneal to 500 K.

results are also consistent with the high stability of oxo species on Mo(110) reported by Colaianni et al.[37]

Thermal desorption data for ^{15}NO (Figure 5) show the high-temperature removal of C, O, and N in three CO and two N_2 desorption peaks. In particular, CO desorption (spectrum c) is observed at approximately 670, 890, and 1066 K, and N_2 desorption (spectrum a), at approximately 760 and 1152 K. As shown by spectrum b in Figure 5, ^{13}C deposited on β-Mo_2C by ethene decomposition at 600 K reacts with oxygen to yield a ^{13}CO desorption peak at ~890 K. The olefin treated surface was not preheated to above 1200 K to drive excess carbon into the subsurface. Hence, we assume that the carbon which is burned off at ~890 K is located in the outermost atomic layer, and we describe it as excess carbon. The thermal desorption data in Figure 6 then imply that dosing a clean β-Mo_2C surface with nitrogen from NO displaces interstitial carbon onto the surface, leading to an increasingly intense CO desorption peak at 600−900 K as the NO exposure is increased. The C(1s) binding energy of excess carbon is determined to be 283.2 eV from synchrotron XPS data (Figure 7) for propene decomposition on β-Mo_2C. For example, annealing the sample to 450−600 K in a 3.4×10^{-9} Torr propene atmosphere leads to a surface characterized by a C(1s) peak at 283.2 eV and a marked attenuation of the interstitial carbon peak at 282.8 eV. Exactly the same result is obtained by dissociating NO on β-Mo_2C. As shown in Figure 8, NO dissociation leads to a surface characterized by a C(1s) binding energy of 283.2 eV. Hence, the results in Figures 6 and 8 directly demonstrate that NO decomposition displaces interstitial carbon onto the carbide surface. This phenomenon is not observed for oxygen adsorption on β-Mo_2C.

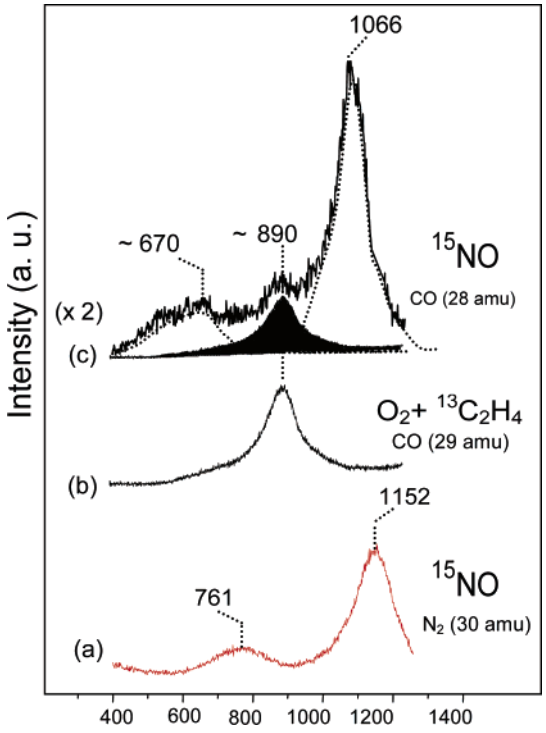

Figure 5. Thermal desorption data for 3 L of ^{15}NO on β-Mo_2C: (a) N_2; (c) CO. Spectrum b displays data for ^{13}CO desorption following $^{13}C_2H_4$ decomposition on oxygen-modified β-Mo_2C.

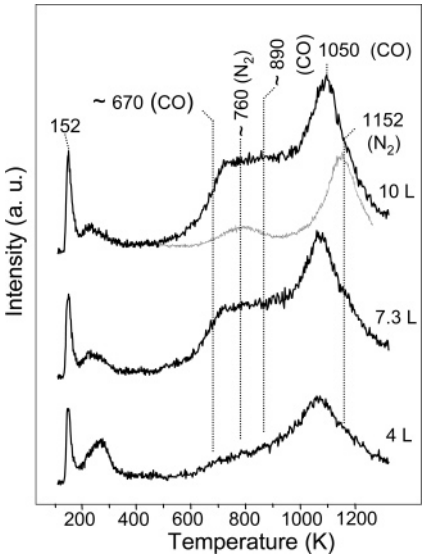

Figure 6. Thermal desorption data (m/e = 28) for ^{14}NO on β-Mo_2C as a function of exposure (4, 7.3, and 10 L). The gray trace under the 10 L spectrum shows reference data for N_2 desorption from experiments using ^{15}NO. These data are included in order to indicate the contribution of N_2 desorption to the m/e = 28 spectra for NO.

Hence, we attribute it to interstitial nitride formation, which is consistent with the free energies of formation of Mo_2C and Mo_2N (−0.09 and −0.52 eV, respectively).[47] As shown in Figure 9, dissociation of NO leads to a new Mo(3d) spin−orbit doublet, at 228.2 and 231.5 eV. Sputter-deposited molybdenum nitride films display Mo(3d) peaks at 228.1 and 231.4 eV in good agreement with these values.[48] Nevertheless, the observed Mo(3d) shifts evidently result from both oxygen and nitrogen deposition.

The N(1s) data in Figure 1 show that there are two types of atomic nitrogen present, a majority state at 397.7 eV and a minority state at 398.3 eV. In contrast to the experiments on

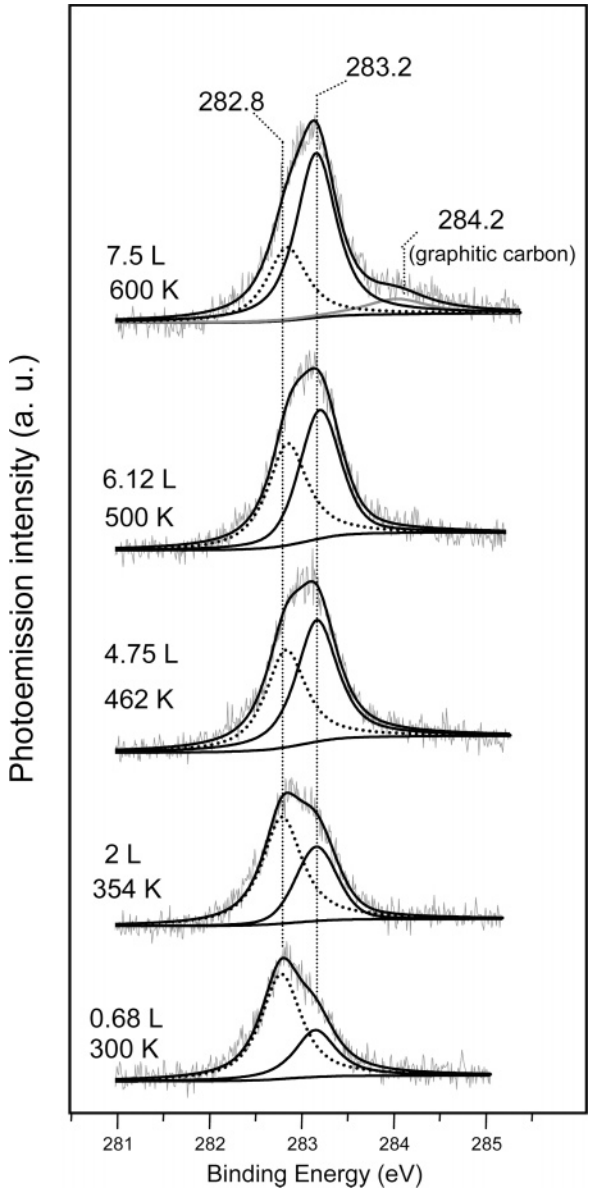

Figure 7. Selected high-resolution C(1s) spectra recorded as a function of continuous exposure of β-Mo_2C to propene (3.4×10^{-9} Torr) during a 0.25 K/s temperature ramp.

atomic oxygen, RAIRS measurements did not provide any information on the atomic nitrogen species (Figure 4). Hence, we tentatively attribute the two N(1s) peaks to interstitial and surface nitrogen, respectively. Recombinative nitrogen desorption is observed (Figure 5) at 761 and 1152 K. These peaks are attributed to the removal of surface and interstitial nitrogen, by analogy to data for recombinative CO desorption from metal carbides. In particular, Brillo et al. reported the removal of surface and carbide carbon from O_2/WC(0001) at 750 and 890 K, respectively.[49] Similarly, the CO desorption peak at approximately 1066 K in Figures 5 and 6 is attributed to the removal of interstitial carbon. CO desorption at ∼1000 K is also observed following CO dissociation on β-Mo_2C. However, the high-temperature CO peak resulting from NO dissociation is much more intense for the same amount of deposited oxygen. Atomic oxygen readily dissolves into clean Mo_2C above 600 K.[6] Hence, the present results suggest that surface nitride serves as a barrier against the diffusion of oxygen into the carbide and leads to an intense high-temperature CO desorption peak. Removal of nitrogen at 1152 K is followed by a return to the stoichiometric Mo_2C surface composition at 1250 K.

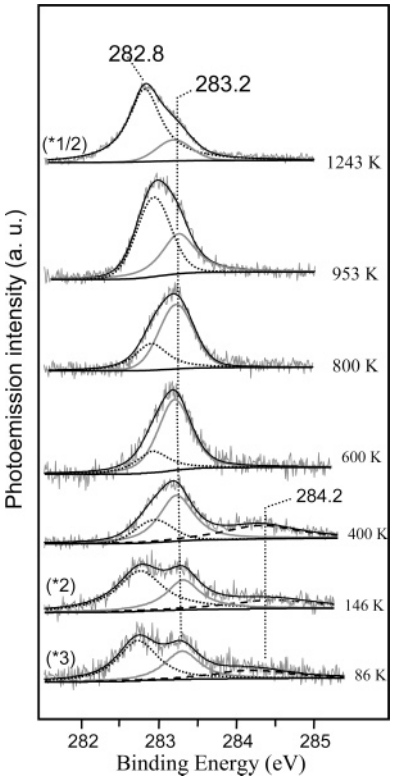

Figure 8. High-resolution C(1s) spectra obtained by progressively annealing the β-Mo_2C surface exposed to 5 L of NO.

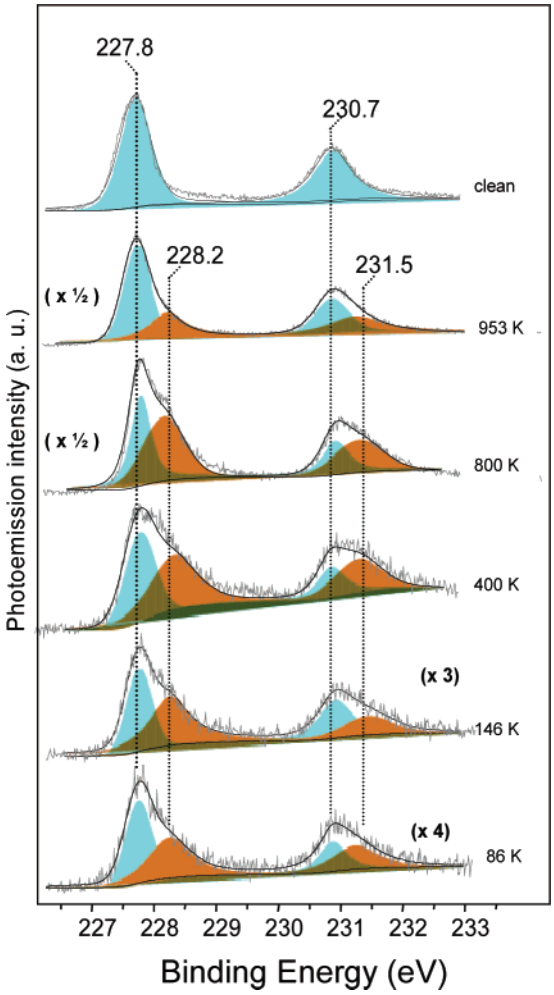

Figure 9. High-resolution Mo(3d) spectra as a function of temperature for 5 L of NO on β-Mo_2C. Peak fitting shows that NO dissociation leads to a new doublet at 228.2 and 231.5 eV.

The key data for the atom-exchange, or displacement, reaction between nitrogen and interstitial carbon are summarized in Figure 10. Figure 10c displays the normalized C(1s) intensities as a function of anneal temperature following the decomposition of NO. Heating the surface exposed to 5 L of NO to 600 K almost completely removes the interstitial carbon C(1s) peak at 282.8 eV and replaces it by a peak at 283.2 eV due to excess carbon. This change is accompanied by a sharp decrease in the N(1s) signal (Figure 10b) in the absence of any desorption peak due to N-containing species (Figure 5). The peak at 283.2 then decreases sharply in the temperature region (800−900 K) coincident with the burnoff of excess carbon (Figures 5 and 6). In contrast, the interstitial carbon peak (282.8 eV) remains constant over the 600−1000 K range and then regains the intensity characteristic of clean β-Mo_2C on heating to 1243 K to desorb N_2 and CO. Heating to above 1200 K is sufficient to establish a stoichiometric surface region regardless of whether the initial surface region is carbon rich or carbon poor. Figure 10a illustrates the following two points: (i) excess carbon can be prepared either by propene decomposition (spectrum a′) or by nitrogen−carbon place exchange (spectrum b′), and (ii) the excess carbon can be eliminated, or greatly attenuated, by heating to 1243 K (spectrum c′). In summary, NO dissociation on β-Mo_2C results in a complex set of compositional changes as the temperature is increased to remove N and O and to heal the surface back to its clean stoichiometric composition. This ability to heal the surface results from the reservoir of carbon provided by the bulk carbide. In a separate publication,[50] we will show that the temperature dependence of the coverage of excess carbon on β-Mo_2C is a key factor in explaining the anomalous thermal stability of alkylidenes on the carbide surface.[4]

The present study helps to clarify the results of a number of XPS investigations of molybdenum carbide. First, several groups have reported slight shifts in the C(1s) spectrum of molybdenum carbide on annealing to high temperatures. For example, a shift of approximately 0.25 eV to lower binding energy was observed on annealing a C/Mo(110) surface, prepared by exposure to 300 L of ethylene at 600 K, to 1200 K.[51] This preparation process developed by Chen and co-workers was found to drive carbon into subsurface sites, thereby increasing the reactivity of the surface to that of Pt-like metals. The data summarized in Figure 10 clearly show that the slight shift in the C(1s) peak may be unambiguously attributed to the removal of excess carbon and the formation of interstitial carbon. Sugihara et al.[52] reported a annealing induced 0.2 eV shift, from 283.1 to 282.9 eV, coincident with a slight decrease in the Mo/C ratio at the surface of α-Mo(0001). Similarly, St-Clair et al.[5] reported that annealing carbon contaminated α-Mo(0001) to 1000 K lead to a 0.1 eV C(1s) shift to lower binding energy. These small shifts are, again, consistent with the removal of excess carbon. Horn et al.[53] recently reported on the deposition of molybdenum carbide nanoparticles on the reconstructed Au(111) surface using a novel method wherein molybdenum was evaporated on multilayer ethylene. Heating above 300 K shifted the C(1s) peak of the nanoparticle from 283.3 to 283.1 eV. In another approach, Kaltchev and Tysoe[54] deposited molybdenum carbide on alumina through the decomposition of adsorbed molybdenum hexacarbonyl. The deposited carbide displayed a C(1s) peak at 283.5 eV. Kaltchev and Tysoe suggested that this high value for the binding energy was due to the presence of a carbidic monolayer rather than a bulk carbide. The present results, as

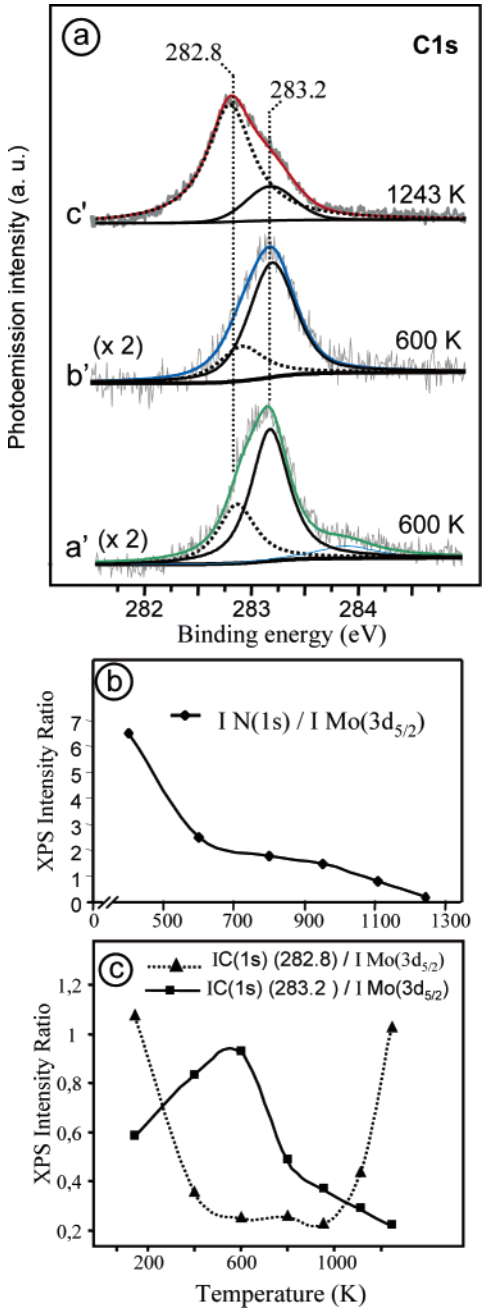

Figure 10. (a) Comparison of the C(1s) spectra at 600 and 1243 K to emphasize the formation of excess carbon by nitrogen−carbon place exchange (a′) or by propene decomposition (b′) and its removal at high temperatures (c′). (b) Normalized integrated N(1s) intensity (sum of the peaks located at 397.7 and 389.3 eV) as a function of temperature for 5 L of NO on β-Mo_2C. (c) Normalized integrated C(1s) intensities as a function of anneal temperature for 5 L of NO on β-Mo_2C.

summarized in Figure 10, support the latter interpretation. Several groups have determined that a carbide phase forms during the induction period for the conversion of methane to benzene over ZSM-5 supported molybdenum particles.[18,19,55] Weckhuysen et al. reported C(1s) data obtained for an active aromatization catalyst following reaction at 1073 K.[55] They observed a graphitic peak at 284.6 eV, a carbide peak at 282.7 eV, and an additional feature at 283.2 eV. They also noted that a peak at the latter binding energy could also be produced by preteatment of the catalyst at 1073 K in CO. Our results indicate that the peak at 283.2 eV is most likely due to excess carbon at the surface. The conclusions of the present study are also relevant to phenomena reported by Xiao et al. for the partial oxidation of methane to synthesis gas on molybdenum carbide catalysts at 1130 K.[56] The latter study revealed the removal of interstitial carbon as CO from the surface region and its replacement by carbon from methane.

Edamoto et al.[57] reported that O_2 dissociation on α-Mo(0001) at room temperature leads to a high-binding-energy shoulder on the carbide C(1s). They attributed this shoulder to a carbon−oxygen interaction. We have also observed a similar shift on exposure of oxygen to clean β-Mo_2C, which we attribute to oxygen bonding to Mo and hence to a modification of the molybdenum carbon interaction. Oxygen adsorption, however, does not displace carbon onto the surface in contrast to the effect of NO described in this publication.

Conclusions

The dissociative adsorption of NO on β-Mo_2C results in the formation of a surface nitride and the displacement of carbide carbon onto the surface. This surface carbon, described as excess carbon, is removed in a CO desorption peak at approximately 850 K. The C(1s) peak binding energy of excess carbon on β-Mo_2C was found to be 283.2 eV. The surface nitride serves as a diffusion barrier against the dissolution of oxygen into the bulk carbide. RAIRS measurements were used to identify surface oxo species resulting from both NO and O_2 dissociation on β-Mo_2C. The study suggests that reactive nitrogen and oxygen codoped molybdenum carbide surfaces may be prepared by exposure to NO followed by annealing to ∼890 K. Failure to anneal to ∼890 K would leave place-exchanged carbon on the surface, thereby rendering the surface relatively inert.

Acknowledgment. We acknowledge support from the Natural Sciences and Engineering Research Council (NSERC) of Canada and from the Fonds Québecois pour la Recherche en Nature et Technologies (FQRNT). We thank Luca Petaccia for technical assistance and R. Rosei for helpful discussions.

References and Notes

(1) Hwu, H. H.; Chen, J. G. *Chem. Rev.* **2005**, *105*, 185.
(2) Siaj, M.; Reed, C.; Oyama, S. T.; Scott, S. L.; McBreen, P. H. *J. Am. Chem. Soc.* **2004**, *126*, 9514.
(3) Siaj, M.; Hassani, H. O.; Zahidi, E.; McBreen, P. H. *Surf. Sci.* **2005**, *579*, 1.
(4) Zahidi, E.; Oudghiri-Hassani, H.; McBreen, P. H. *Nature* **2001**, *409*, 1023.
(5) St. Clair, T. P.; Oyama, S. T.; Cox, D. F.; Otani, S.; Ishizawa, Y.; Lo, R.-L.; Fukui, K.-I.; Iwasawa, Y. *Surf. Sci.* **1999**, *426*, 187.
(6) St. Clair, T. P.; Oyama, S. T.; Cox, D. F. *Surf. Sci.* **2000**, *468*, 62.
(7) St. Clair, T. P.; Oyama, S. T.; Cox, D. F. *Surf. Sci.* **2002**, *511*, 294.
(8) Chen, J. G. *Chem. Rev.* **1996**, *96*, 1477.
(9) Hwu, H. H.; Zellner, M. B.; Chen, J. G. *J. Catal.* **2005**, *229*, 30.
(10) Levy, R. L.; Boudart, M. *Science* **1973**, *181*, 547.
(11) Frühberger, B.; Chen, J. G. *J. Am. Chem. Soc.* **1996**, *118*, 11599.
(12) Oyama, S. T., Ed. *The Chemistry of Transition Metal Carbides and Nitrides*; Blackie Academic and Professional: Glasgow, Scotland, 1996.
(13) Hanif, A.; Xiao, T. C.; York, A. P. E.; Sloan, J.; Green, M. L. H. *Chem. Mater.* **2002**, *14*, 1009.
(14) St. Clair, T. P.; Dhandapani, B.; Oyama, S. T. *Catal. Lett.* **1999**, *58*, 169.
(15) Choi, J. S.; Krafft, J.-M.; Krzton, A.; Djèja-Mariadassou, G. *Catal. Lett.* **2002**, *81*, 175.
(16) Choi, J. S.; Bugli, G.; Djèja-Mariadassou, G. *J. Catal.* **2000**, *193*, 238.
(17) Xiao, T.; York, A. P. E.; Coleman, K. S.; Claridge, J. B.; Sloan, J.; Charnock, J.; Green, M. L. H. *J. Mater. Chem.* **2001**, *11*, 3094.
(18) Ding, W.; Liu, S.; Meitzner, G. D.; Iglesia, E. *J. Phys. Chem. B* **2001**, *105*, 506.
(19) Liu, S.; Wang, L.; Ohnishi, R.; Ichikawa, K. *J. Catal.* **1999**, *181*, 175.
(20) Liu, P.; Rodriguez, J. A. *J. Chem. Phys.* **2004**, *120*, 5414.
(21) Pham-Huu, C.; Ledoux, M. J.; Guille, J. *J. Catal.* **1993**, *143*, 249.

(22) Iglesia, E.; Baumgartner, J. E.; Ribeiro, J. E.; Boudart, M. *J. Catal.* **1991**, *131*, 523.
(23) Frantz, P.; Didziulis, S. V. *Surf. Sci.* **1998**, *412*−*413*, 384.
(24) Merrill, P. B.; Perry, S. S.; Frantz, P.; Didziulis, S. V. *J. Phys. Chem. B* **1998**, *102*, 7606.
(25) Souda, R.; Aizawa, T.; Otani, S.; Ishizawa, Y.; Oshima, C. *Surf. Sci.* **1991**, *256*, 19.
(26) Wang, J.; Castonguay, M.; Deng, J.; McBreen, P. H. *Surf. Sci.* **1997**, *374*, 197.
(27) Oudghiri-Hassani, H.; Zahidi, E.; Siaj, M.; Wang, J.; McBreen, P. H. *Appl. Surf. Sci.* **2003**, *212*−*213*, 4.
(28) Brillo, J.; Sur, R.; Kuhlenbeck, H.; Freund, H.-J. *Surf. Sci.* **1998**, *397*, 137.
(29) Zhang, M. H.; Hwu, H. H.; Buelow, M. T.; Chen, J. G.; Ballinger, T. H.; Andersen, P. J. *Catal. Lett.* **2001**, *77*, 29.
(30) Zhang, M. H.; Hwu, H. H.; Buelow, M. T.; Chen, J. G.; Ballinger, T. H.; Andersen, P. J.; Mullins, D. R. *Surf. Sci.* **2003**, *522*, 112.
(31) Wang, J.; Castonguay, M.; McBreen, P. H.; Ramanathan, S.; Oyama, S. T. *The Chemistry of Transition Metal Carbides and Nitrides*; Blackie Academic and Professional: Glasgow, Scotland, 1996; Chapter 23.
(32) Baraldi, A.; Barnaba, M.; Brena, B.; Cocco, D.; Comelli, G.; Lizzit, S.; Paolucci, G.; Rosei, R. *J. Electron Spectrosc. Relat. Phenom.* **1995**, *76*, 145.
(33) Zhu, J. F.; Kinne, M.; Fuhrmann, T.; Denecke, R.; Steinrück, H.-P. *Surf. Sci.* **2003**, *529*, 384.
(34) Lizzit, S.; Baraldi, A.; Cocco, D.; Comelli, G.; Paolucci, G.; Rosei, R.; Kiskinova, M. *Surf. Sci.* **1998**, *410*, 228.
(35) Birchem, T.; Muhler, M. *Surf. Sci.* **1995**, *334*, L701.
(36) Stefanov, P.; Marinova, T. *Surf. Sci.* **1988**, *200*, 26.
(37) Colaianni, M. L.; Chen, J. G.; Weinberg, W. H.; Yates, J. T. J. *Surf. Sci.* **1992**, *279*, 211.
(38) Kim, S. H.; Stair, P. C. *Surf. Sci.* **2000**, *457*, L437.
(39) Street, S. C.; Liu, G.; Goodman, D. W. *Surf. Sci.* **1997**, *385*, L971.
(40) T. Sasaki, Y.; Goto, R.; Tero, K.-I. F.; Iwasawa, Y. *Surf. Sci.* **2002**, *502*−*503*, 136.
(41) Nart, F. C.; Friend, C. M. *J. Phys. Chem. B* **2001**, *105*, 2773.
(42) Nart, F. C.; Kelling, S.; Friend, C. M. *J. Phys. Chem. B* **2000**, *104*, 3212.
(43) Deiner, L. J.; Serafin, J. G.; Friend, C. M.; Weller, S. G.; Levinson, J. A.; Palmer, R. E. *J. Am. Chem. Soc.* **2003**, *125*, 13252.
(44) Basu, P.; Nemykin, V. N.; Sengar, R. S. *Inorg. Chem.* **2003**, *42*, 7489.
(45) Edamoto, K.; Sugihara, M.; Ozawa, K.; Otani, S. *Surf. Sci.* **2004**, *561*, 101.
(46) Chan, A. S. Y.; Deiner, L. J.; Friend, C. M. *J. Phys. Chem. B* **2002**, *106*, 13318.
(47) Galasso, F. S. *Structure and Properties of Inorganic Solids*; Pergamon: Oxford, U.K., 1970.
(48) Shen, Y. G. *Mater. Sci. Eng., A* **2003**, *359*, 158.
(49) Brillo, J.; Kuhlenbeck, H.; Freund, H.-J. *Surf. Sci.* **1998**, *409*, 199.
(50) Siaj, M.; Oudghiri-Hassani, H.; Zahidi, E.; Maltais, C.; McBreen, P. H. Manuscript in preparation.
(51) Frühberger, B.; Chen, J. G.; Eng, J. J.; Bent, B. E. *J. Vac. Sci. Technol., A* **1996**, *14*, 1475.
(52) Sugihara, M.; Ozawa, K.; Edamoto, K.; Otani, S. *Solid State Commun.* **2002**, *121*, 1.
(53) Horn, J. M.; Song, Z.; Potapenko, D. V.; Hrbek, J.; White, M. G. *J. Phys. Chem. B* **2005**, *109*, 44.
(54) Kaltchev, M.; Tysoe, W. T. *J. Catal.* **2000**, *193*, 29.
(55) Weckhuysen, B. M.; Rosynek, M. P.; Lunsford, J. H. *Catal. Lett.* **1998**, *52*, 31.
(56) Xiao, C.-T.; Hanif, A.; York, A. P. E.; Nishizaka, Y.; Green, M. L. H. *Phys. Chem. Chem. Phys.* **2002**, *4*, 4549.
(57) Edamoto, K.; Sugihara, M.; Ozawa, K.; Otani, S. *Appl. Surf. Sci.* **2004**, *237*, 498.